Journal of Computer Science and Cybernetics, V.40, N.3 (2024), 267-286
DOI: 10.15625/1813-9663/19558

ADAPTIVE NEURAL PATH-FOLLOWING CONTROL OF UNDER-ACTUATED AUV SUBJECT TO SYSTEM UNCERTAINTIES AND INPUT CONSTRAINTS

PHAM NGUYEN NHUT THANH[1,2], HO PHAM HUY ANH[1,2,*]

[1] *Ho Chi Minh City University of Technology (HCMUT), 268 Ly Thuong Kiet Street, District 10, Ho Chi Minh City, Viet Nam*
[2] *Vietnam National University Ho Chi Minh City (VNU-HCM), Linh Trung Ward, Thu Duc District, Ho Chi Minh City, Viet Nam*

Abstract. This paper investigates a path-following control for autonomous underwater vehicles that is underactuated and subject to system uncertainties and input constraints in the vertical plane. Initially, the-line-of sight guidance is adopted to generate the desired pitch angle and the updated law for the path variable to guide the vehicle toward the desired path. Subsequently, a transformation is applied to turn the input constraints into a constraint on new states. The state constraint problem, unknown parameters, and disturbances are then addressed with the proposal of an innovative integral barrier Lyapunov function and adaptive law. Through the Lyapunov theory, all errors are shown to be uniformly ultimately bounded. Eventually, a simulation via Matlab is implemented to illustrate the feasibility and efficiency of the designed controller.

Keywords. Adaptive neural path-following, autonomous underwater vehicles (AUVs), under-actuated system, integral barrier Lyapunov function (IBLF), input constraints.

1. INTRODUCTION

As a leading tool in the ocean exploitation trend, autonomous underwater vehicles (AUVs) are researched extensively to serve applications such as pipeline inspection, seafloor mapping, and new resource exploration [1, 2, 3]. The common characteristic of this type of vehicle is under-actuated, which means the actuators equipped on the vehicles are fewer than the degrees of freedom to be controlled. Along with unpredictable disturbances of the ocean environment, this characteristic makes developing robust and efficient controllers really challenging for researchers. To execute these undersea tasks, AUVs are often required to follow a pre-assigned trajectory. Moreover, depending on whether there is a coupling between kinematic and dynamic or not in the control objective, it will be classified into path-following or trajectory-tracking problems [4, 5].

The path-following control problem for AUVs has been widely researched, and many advanced approaches and algorithms have been developed over the past decades [6, 7, 8, 9]. For example, to create a path-following controller with high robustness against uncertainties

*Corresponding author.
E-mail addresses: pnnthanh.sdh21@hcmut.edu.vn (P.N.N Thanh); hphanh@hcmut.edu.vn (H.P.H Anh).

for AUV, Lyapunov, backstepping, and hybrid parameter adaptive techniques were adopted [6]. In [7], the authors utilized the Lagrange multipliers to solve the path-following control problem for underwater vehicles. Yu et al. [8] incorporated a fuzzy strategy into sliding mode control to achieve a hybrid controller that guides a bio-inspired robotic dolphin in vertical motion. In [9], singular perturbation theory was adopted to stabilize AUV to a pre-assigned path in the longitudinal plane. However, the line of sight (LOS) algorithm is the most popular for marine vehicles because of its simplicity and intuitiveness. Specifically, LOS guidance mimics an experienced helmsman to effectively regulate the vehicle to converge to a desired path. For that reason, many studies have applied and developed different modifications of LOS for the path-following problem, including, but not limited to, integral LOS [10, 11], adaptive LOS [12, 13, 14], and composite LOS [15, 16].

It should be pointed out that after using the LOS guidance to derive the desired kinematic values, the dynamic layer needs to guarantee that the corresponding state of the vehicle adheres to these desired values. However, the above-mentioned articles often build model-based dynamic controllers, causing two critical problems. The primary problem is that the model-based controller requires the model parameters, which are difficult to determine precisely [6, 17]. Hence, to maintain the control performance, augmenting with an observer [15, 18, 19] or making use of the strong learning characteristics of the fuzzy logic system (FLS) and neural network (NN) [11, 12, 14] is required. The secondary problem relates to the physical limitations of the actual model, which can affect the performance and stability of the controller when applied in practice [11, 20]. The physical limitations include actuator saturation and state constraint. Actuator saturation is inherent in many mechanical systems, which results in performance degradation or instability when the command signals exceed the actual ones. In [21], a novel saturation function on the interval $(0, 1]$ was developed to address the unknown asymmetrical input constraint. In [20, 22], the actuator dynamic model was taken into account during the controller design process to improve the practical viability of the suggested control scheme. However, they used a first-order differential equation to describe the actuator dynamics, which imposes the changing rate of output signals through a time constant and ignores the actuator rate constraint. Regarding the state constraint, since the providing control inputs are bounded, the velocities of AUVs are passively bounded [4, 14]. To overcome this problem, Peng et al. [4] adopted a projection neural network and reference governor to ensure that the vehicle's velocities remain in the given constraint. In [14], a modified barrier Lyapunov function was proposed to achieve state constraint satisfaction.

From the above observations, this paper attempts to build an adaptive path-following controller for autonomous underwater vehicles subject to system uncertainties, actuator saturations, and state constraints. The following is a list of the paper's primary contributions.

(i) Instead of using a first-order differential equation to approximate the actuator dynamic [20, 22], this paper uses a transformation to transform the actuator saturation problem into a state constraint one. After that, a novel integral barrier Lyapunov function (IBLF) is proposed to ensure that there is never a violation of any constraint.

(ii) Different from previous studies, we use the radial basis function (RBF) NN and IBLF to construct a model-free control law that relaxes the model information requirements and thus overcomes the disadvantages of the model-based approach. Moreover, an adaptive law is integrated into the control law to compensate for the approximation errors and

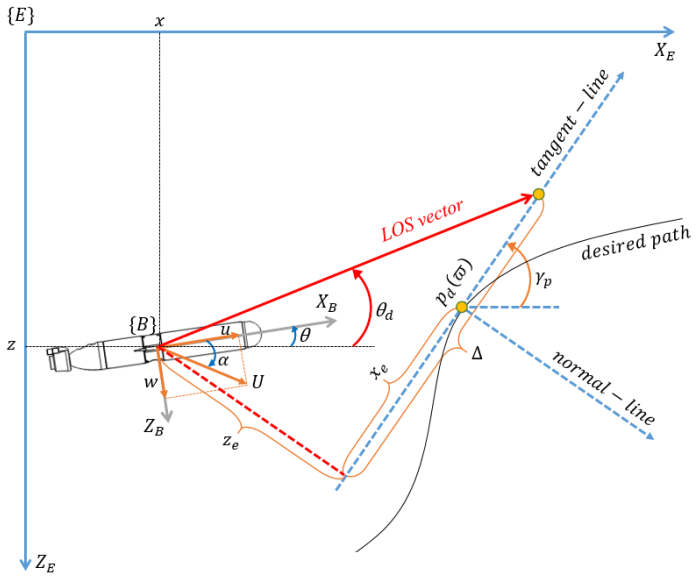

Figure 1: Geometric of LOS guidance

lumped disturbance. The stability of the proposed controller is demonstrated through theoretical analysis and simulation results.

The subsequent sections comprise the remainder of this paper. Section 2 introduces the AUV mathematical model and control objective. Section 3 details the proposed controller design procedure. Section 4 discusses the simulation results of the proposed controller. Finally, Section 5 concludes the paper.

2. MATHEMATICAL MODEL AND PROBLEM FORMULATION

2.1. Mathematical model

This section introduces the AUV model investigated in the study [18, 23], which has the simplified kinematic and dynamic models in the vertical plane as follows

$$\begin{cases} \dot{x} = u\cos\theta + w\sin\theta \\ \dot{z} = -u\sin\theta + w\cos\theta \\ \dot{\theta} = q, \end{cases} \tag{1}$$

$$\begin{cases} \dot{u} = f_u + g_u T_p + d_u \\ \dot{w} = f_w + d_w \\ \dot{q} = f_q + g_q x_G + d_q, \end{cases} \tag{2}$$

where $[x, y, \theta]^\top$ is the position and pitch angle of AUV in the earth-fixed frame $\{E\}$, $[u, w, q]^\top$ respectively represent the surge, heave velocities, and pitch rate in the body-fixed frame $\{B\}$ (see Figure 1). The continuous functions f_i, g_i, $i = u, w, q$ are given in Eq.(3a) to Eq.(3e),

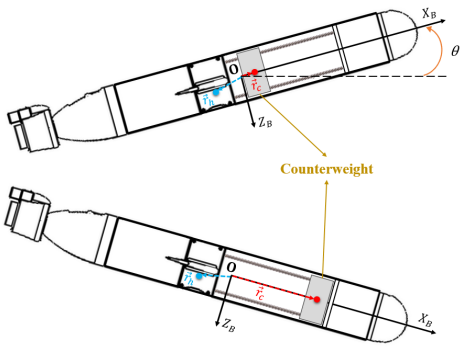

Figure 2: The counterweight mechanism

d_i is lumped by linearization errors and external disturbances.

$$f_u = \frac{(Z_{\dot{w}} - m)\, wq + (Z_{\dot{q}} + mx_G)\, q^2 + X_{uu} u\,|u| - (W - B)\sin\theta}{m - X_{\dot{u}}}, \tag{3a}$$

$$f_w = \frac{(m - X_{\dot{u}} + Z_{uqf})\, uq + Z_{ww} w\,|w| + Z_{qq} q\,|q|}{m - Z_{\dot{w}}} + \frac{mz_G q^2 + (Z_{uwl} + Z_{uwf})\, uw + (W - B)\cos\theta}{m - Z_{\dot{w}}}, \tag{3b}$$

$$f_q = \frac{(X_{\dot{u}} - Z_{\dot{w}} + M_{uwl} + M_{uwf})\, uw + M_{ww} w\,|w|}{I_{yy} - M_{\dot{q}}} + \frac{-mz_G wq + M_{qq} q\,|q| + (M_{uqf} - Z_{\dot{q}})\, uq - z_G W\sin\theta}{I_{yy} - M_{\dot{q}}}, \tag{3c}$$

$$g_u = \frac{1}{m - X_{\dot{u}}}, \tag{3d}$$

$$g_q = -\frac{muq + W\cos\theta}{I_{yy} - M_{\dot{q}}}, \tag{3e}$$

where $X_{(.)}$, $Z_{(.)}$, $M_{(.)}$ are the hydrodynamic parameters of the AUV, m and W are the total mass and weight of the vehicle, while B and I_{yy} are the buoyancy and the inertial moment, respectively. Besides, the control inputs acting on AUV include T_p being the thrust force from the thruster and x_G being the x-coordinate of the center of gravity (CG) on $\{B\}$. Different from the conventional AUV, the AUV considered in this paper uses a counterweight mechanism to control the pitch channel via shifting the counterweight along the $x - axis$, as shown in Figure 2.

The counterweight mechanism consists of four guild rails that allow adjusting the position of the counterweight [18] while the mass of the counterweight m_c will be distributed so that its center of gravity in $\{B\}$ is $r_c = [x_c, 0, 0]^\top$. Denote $m_h = m - m_c$ is the vehicle's weight without the counterweight, and $r_h = [r_{hx}, r_{hy}, r_{hz}]^\top$ is the corresponding coordinate of its center of gravity in $\{B\}$. Then, the relationship between the coordinates of the vehicle's CG and the counterweight can be described by the following formula

$$r_G = [x_G, y_G, z_G]^\top = \frac{m_h r_h + m_c r_c}{m_h + m_c} = \left[\frac{m_h r_{hx} + m_c x_c}{m}, \frac{m_h r_{hy}}{m}, \frac{m_h r_{hz}}{m}\right]^\top. \tag{4}$$

It can be observed from equation (4) that changing the counterweight position x_c will only affect x_G, which is also the control input for the pitch angle. Nevertheless, the displacement and the moving speed of the counterweight are physically limited. From the relationship of x_G and x_c in (4), we can rewrite the pitch channel in (2) as follows

$$\dot{q} = f_c + g_c x_c + d_q, \tag{5}$$

where $f_c = f_q + g_q m_h r_{hx}/m$, $g_c = g_q m_c/m$. Representation (5) allows us to directly analyze and address the problem of constraints on control input x_c, which is also known as the magnitude and rate constraints (MRC) mentioned in [24, 25]. Moreover, the constraint on control input also renders the constraint of the related states [14]. In this paper, we use the following conditions to formulate this problem.

$$\begin{cases} -k_{lM} < x_c < k_{uM} \\ -k_{lR} < \dot{x}_c < k_{uR} \\ -k_{l\theta} < \theta < k_{u\theta} \\ -k_{lq} < q < k_{uq}, \end{cases} \tag{6}$$

where positive constants k_{li}, k_{ui} $(i = M, R, \theta, q)$ stand for the lower and upper limitations of the corresponding state.

2.2. Problem formulation

In many practical underwater applications, AUVs are required to move along a predetermined path to fulfill the tasks, such as pipeline exploration and seabed surveys. Assume that the desired path in the vertical plane is parameterized by $p_d(\varpi) = [x_d(\varpi), z_d(\varpi)]^\top$, where $\varpi \in \mathbb{R}$ is the path variable, as shown in Figure 1. Then, the control problem that regulates the vehicle to converge to the desired path can be converted into designing the control law so that the along-track error x_e and the cross-track error z_e settle down in the vicinity of zero. According to [4, 23], these error variables can be determined through the following formula

$$\begin{cases} x_e = (x - x_d(\varpi)) \cos\gamma_d - (z - z_d(\varpi)) \sin\gamma_d \\ z_e = (x - x_d(\varpi)) \sin\gamma_d + (z - z_d(\varpi)) \cos\gamma_d, \end{cases} \tag{7}$$

where $\gamma_d = \arctan(-z'_d(\varpi)/x'_d(\varpi))$, $x'_d(\varpi)$ and $z'_d(\varpi)$ are partial derivatives of $x_d(\varpi)$ and $z_d(\varpi)$ with respect to ϖ. For clearing, the control objective can be expressed as below.

Control objective: Design the control law for x_c satisfying the constraints (6) and the updated law for ϖ so that the path-following errors (7) settle to a neighborhood of zero regardless of system uncertainties, i.e., functions f_i and g_i are unknown, and external disturbances.

To accomplish the control objective, the below assumptions are required.

Assumption 1. *The lumped disturbances d_i $(i = u, w, q)$ are unknown but bounded. Hence, there exist positive constants $\bar{d}_i$ such that $|d_i| \leqslant \bar{d}_i$.*

Assumption 2. *The surge velocity u satisfies $0 < u \leqslant U_0$.*

Assumption 3. *[26] The function g_c satisfies $\bar{g}_c < g_c < 0$, where $\bar{g}_c$ is a known function.*

Assumption 4. *The desired trajectory and its first and second derivatives are bounded.*

Remark 1. *In this study, we assume that the thrust force T_p acting on the vehicle is constant [18, 27]. This is because the propeller velocity is fixed to compensate for the roll offset. Besides, since both control inputs and the energy of ocean disturbances are limited, Assumptions 1 - 2 are reasonable. Assumption 3 indicates that the sign of the control gain g_c and the upper bound of $|g_c|$ are known, while the actual value is not required for the controller design.*

2.3. Related lemmas

Lemma 1. *Consider the integral barrier Lyapunov function (IBLF) for a state-constrained $-k_l < s < k_u$ as*

$$I(e,\omega) = \int_0^e \frac{\beta\sigma(k_l+k_u)^2}{4(k_l+\sigma+\omega)(k_u-\sigma-\omega)}d\sigma, \tag{8}$$

where k_l, $k_u > 0$, $e = s-\omega$ with ω is the desired value of s and satisfies $-k_l < \omega < k_u$, $\beta(s)$ is a continuous function satisfying $1 \leqslant \beta \leqslant \bar{\beta}$ with $\bar{\beta}$ as an unknown positive constant yet bounded. Then, the following properties hold.

(i) The derivative of $I(e,\omega)$ with respect to time is $\dot{I}(e,\omega) = e(\beta\lambda_s\dot{s} - \rho(e,\omega)\dot{\omega})$, where $\lambda_s = \frac{(k_l+k_u)^2}{4(k_l+s)(k_u-s)}$ and $\rho(e,\omega) = \int_0^1 \frac{\beta(\xi e+\omega)(k_l+k_u)^2}{4(k_l+\xi e+\omega)(k_u-\xi e-\omega)}d\xi$.

(ii) The $\rho(e,\omega)$ is well-defined when e approaches zero.

(iii) The IBLF satisfies $\frac{1}{2}e^2 \leqslant I(e,\omega) \leqslant \bar{\beta}\lambda_s e^2$.

Proof.

(i) According to [26, 28], we have

$$\begin{aligned}\dot{I}(e,\omega) &= \frac{\beta e(k_l+k_u)^2}{4(k_l+e+\omega)(k_u-e-\omega)}\dot{e} + \frac{\partial I(e,\omega)}{\partial\omega}\dot{\omega} \\ &= \beta e\lambda_s\dot{e} + \frac{\partial I(e,\omega)}{\partial\omega}\dot{\omega}\end{aligned} \tag{9}$$

and

$$\begin{aligned}\frac{\partial I(e,\omega)}{\partial\omega} &= \frac{\beta(\sigma+\omega)\sigma(k_l+k_u)^2}{4(k_l+\sigma+\omega)(k_u-\sigma-\omega)}\Bigg|_0^e - e\int_0^1 \frac{\beta(\xi e+\omega)(k_l+k_u)^2}{4(k_l+\xi e+\omega)(k_u-\xi e-\omega)}d\xi \\ &= \beta e\lambda_s - e\rho(e,\omega).\end{aligned} \tag{10}$$

Combining (9) - (10) and note that $\dot{e} = \dot{s} - \dot{\omega}$, we get the conclusion.

(ii) It can be observed that $\rho(0,\omega) = \frac{\beta(\omega)(k_l+k_u)^2}{4(k_l+\omega)(k_u-\omega)}$, which shows that $\rho(e,\omega)$ is well-defined as $-k_l < \omega < k_u$.

(iii) Using the variable change $\sigma = \xi e$, we obtain

$$I(e,\omega) = e^2 \int_0^1 \frac{\beta(\xi e+\omega)\,\xi(k_l+k_u)^2}{4(k_l+\xi e+\omega)(k_u-\xi e-\omega)} d\xi.$$

Based on the definition of β and Cauchy-Schwarz inequality, we have

$$\begin{cases} \beta(\xi e+\omega) \geqslant 1 \\ \dfrac{(k_l+k_u)^2}{4(k_l+\xi e+\omega)(k_u-\xi e-\omega)} \geqslant \dfrac{(k_l+k_u)^2}{(k_l+\xi e+\omega+k_u-\xi e-\omega)^2} = 1. \end{cases}$$

Hence

$$I(e,\omega) \geqslant e^2 \int_0^1 \xi d\xi = \frac{e^2}{2}. \tag{11}$$

Let $p(\sigma,\omega) = \frac{\sigma(k_l+k_u)^2}{4(k_l+\sigma+\omega)(k_u-\sigma-\omega)}$. We have

$$\frac{\partial p(\sigma,\omega)}{\partial \sigma} = \frac{(k_l+k_u)^2\left[\sigma^2+(k_l+\omega)(k_u-\omega)\right]}{4(k_l+\sigma+\omega)^2(k_u-\sigma-\omega)^2},$$

which shows that $\partial p(\sigma,\omega)/\partial\sigma > 0$ on $-k_l < \sigma+\omega < k_u$. Hence, $p(\sigma,\omega)$ is a monotonically increasing function with σ. Using the mean value theorem and note that $p(0,\omega) = 0$, $\beta \leqslant \bar{\beta}$, we obtain

$$I(e,\omega) = \int_0^e \beta p(\sigma,\omega)\, d\sigma \leqslant e\bar{\beta} p(e,\omega) = \bar{\beta}\lambda_s e^2. \tag{12}$$

Combining (11)-(12), we get the conclusion. ∎

Remark 2. *Compared to [29], the IBLF (8) is more general with the appearance of β, which is the key to building our proposed control laws when g_c is unknown. Besides, in the case of $\beta = 1$, we can easily obtain [29]*

$$\dot{I}(e,\omega) = e(\lambda_s \dot{s} + \kappa_s \dot{\omega}), \tag{13}$$

where $\kappa_s = \frac{k_l+k_u}{4e} \ln \frac{(k_l+\omega)(k_u-e-\omega)}{(k_u-\omega)(k_l+e+\omega)}$.

Lemma 2. *[30] Given an unknown continuous function $f(\zeta)$ on compact set $\Omega \in \mathbb{R}^n$ and a positive constant $\bar{\varepsilon}$. The RBF neural network can approximate $f(\zeta)$ by*

$$f(\zeta) = W^\top S(\zeta) + \varepsilon, \tag{14}$$

where W is the ideal weight vector, $S(\zeta)$ is the vector containing activation functions, and ε is the error of function approximation such that $|\varepsilon| \leqslant \bar{\varepsilon}$.

Lemma 3. *[31] Given any $\varsigma > 0$ and $x \in \mathbb{R}$, the following inequalities hold*

$$0 \leqslant |x| - x\tanh\left(\frac{x}{\varsigma}\right) \leqslant \eta\varsigma, \tag{15}$$

where $\eta = 0.2785$.

3. PROPOSED CONTROLLER

This section will elaborate on a controller design procedure to achieve the control objective through the two sequential steps. Step 1, the LOS guidance law will be applied to generate the updated law for ϖ and a desired pitch angle θ_d^c. The former will ensure that the normal line of point $p_d(\varpi)$ on the path always passes through the origin of $\{B\}$, while the latter will steer the ship toward the desired path. In step 2, the constraint control method based on BLF is cleverly utilized to design a control law to make the vehicle's pitch angle adhere to the desired one while guaranteeing the constraints are never violated.

3.1. LOS-based guidance law

Differentiating the path-following errors (7) with respect to time and combining with (1) yields

$$\begin{aligned}\dot{x}_e &= (\dot{x} - \dot{x}_d(\varpi))\cos\gamma_d - (\dot{z} - \dot{z}_d(\varpi))\sin\gamma_d - \dot{\gamma}_d z_e \\ &= (u\cos\theta + w\sin\theta)\cos\gamma_d - (-u\sin\theta + w\cos\theta)\sin\gamma_d - U_d\dot{\varpi} - \dot{\gamma}_d z_e \\ &= U\cos(\theta - \gamma_d - \alpha) - U_d\dot{\varpi} - \dot{\gamma}_d z_e,\end{aligned} \tag{16}$$

$$\begin{aligned}\dot{z}_e &= (\dot{x} - \dot{x}_d(\varpi))\sin\gamma_d + (\dot{z} - \dot{z}_d(\varpi))\cos\gamma_d + \dot{\gamma}_d x_e \\ &= (u\cos\theta + w\sin\theta)\sin\gamma_d + (-u\sin\theta + w\cos\theta)\cos\gamma_d + \dot{\gamma}_d x_e \\ &= -U\sin(\theta - \gamma_d - \alpha) + \dot{\gamma}_d x_e,\end{aligned} \tag{17}$$

where $U = \sqrt{u^2 + w^2}$, $U_d = \sqrt{x_d'^2(\varpi) + z_d'^2(\varpi)}$, $\alpha = \arctan(w, u)$. From (16) - (17), we proposed the LOS-based guidance law as follows

$$\dot{\varpi} = \frac{k_1 x_e + U\cos(\theta - \gamma_d - \alpha)}{U_d}, \tag{18a}$$

$$\theta_d^c = \gamma_d + \alpha + \chi, \tag{18b}$$

where $k_1 > 0$, $\chi = \operatorname{atan}(z_e/\Delta)$ with $\Delta > 0$. Let $\tilde{\theta} = \theta - \theta_d^c$ and define the first Lyapunov function as $V_1 = \left(x_e^2 + z_e^2\right)/2$. Taking the time derivative of V_1 along with (16) - (18b), we obtain

$$\begin{aligned}\dot{V}_1 &= x_e\left(U\cos(\theta - \gamma_d - \alpha) - U_d\dot{\varpi} - \dot{\gamma}_d z_e\right) + z_e\left(-U\sin(\theta - \gamma_d - \alpha) + \dot{\gamma}_d x_e\right) \\ &= x_e\left(U\cos(\theta - \gamma_d - \alpha) - U_d\dot{\varpi}\right) - U z_e\sin(\theta - \gamma_d - \alpha) \\ &= -k_1 x_e^2 - U z_e\sin\left(\tilde{\theta} + \chi\right) \\ &= -k_1 x_e^2 - U z_e\sin\chi + U z_e\tilde{\theta}\left(\sin\chi\frac{1 - \cos\tilde{\theta}}{\tilde{\theta}} - \cos\chi\frac{\sin\tilde{\theta}}{\tilde{\theta}}\right) \\ &= -k_1 x_e^2 - k_2 z_e^2 + z_e\tilde{\theta}U\varphi\left(\tilde{\theta}, \chi\right),\end{aligned} \tag{19}$$

where $k_2 = \frac{U}{\sqrt{z_e^2 + \Delta}} > 0$, $\varphi\left(\tilde{\theta}, \chi\right) = \sin\chi\frac{1 - \cos\tilde{\theta}}{\tilde{\theta}} - \cos\chi\frac{\sin\tilde{\theta}}{\tilde{\theta}}$.

Remark 3. *The term $\varphi\left(\tilde{\theta}, \chi\right)$ is bounded, i.e., $\left|\varphi\left(\tilde{\theta}, \chi\right)\right| \leqslant 1$, and thus can be used to design the control law in the next step.*

3.2. BLF-based pitch controller

From (19), it is evident that if $\tilde{\theta}$ converges to zero, the path-following errors settle to a neighborhood of zero. Hence, the goal of this section is to build a robust control law x_c to stabilize $\tilde{\theta}$ while complying with the physical limitations (6). To this end, we first introduce new variables to transform the MRC problem into a state-constrained problem.

$$\begin{cases} x_c(t) = x_c(0) + \int_0^t \vartheta dt \\ \vartheta(t) = \dot{x}_c(0) + \int_0^t \tau dt \end{cases} \Rightarrow \begin{cases} \dot{x}_c = \vartheta \\ \dot{\vartheta} = \tau, \end{cases} \tag{20}$$

where $x_c(0)$ and $\dot{x}_c(0)$ are the initial values of x_c and $\dot{x}_c$, respectively. Then, ϑ and τ can be considered as the counterweight's speed and new free control input. Next, dynamic surface control (DSC) is employed to attenuate the complexity of the virtual control derivative operation in the traditional backstepping technique. Specifically, the virtual control variable ω^c will be passed through the following saturation filter [29]

$$T_s\dot{\omega} + \omega = H_s(\omega^c), \omega(0) = H_s(\omega^c(0)), \tag{21}$$

$$H_s(\omega^c) = \begin{cases} -k_{ls} + \mu_f & \text{if} \quad \omega^c < -k_{ls} + \mu_f \\ k_{us} - \mu_f & \text{if} \quad \omega^c > -k_{ls} + \mu_f \\ \omega^c & \text{otherwise,} \end{cases} \tag{22}$$

with k_{ls}, k_{us} are the lower and upper limitations of the corresponding state, T_s, μ_f are adjustable positive constants. By doing so, the filtered virtual control variable ω are guaranteed to be continuous and remain within the given constraints (6).

Since the pitch angle is a constrained state, we let θ_d^c pass through the filter (21) to achieve θ_d and utilize the IBLF for it as $V_2 = \int_0^{e_\theta} \frac{\sigma(k_{l\theta}+k_{u\theta})^2}{4(k_{l\theta}+\sigma+\theta_d)(k_{u\theta}-\sigma-\theta_d)} d\sigma$ with $e_\theta = \theta - \theta_d$. Using Remark 2, the derivative of V_2 is given as

$$\dot{V}_2 = e_\theta \left(\lambda_\theta q + \kappa_\theta \dot{\theta}_d\right). \tag{23}$$

Select the virtual control law as

$$q_d^c = -k_3 e_\theta - \frac{\kappa_\theta}{\lambda_\theta}\dot{\theta}_d - \frac{1}{\lambda_\theta} z_e U \varphi\left(\tilde{\theta}, \chi\right), \tag{24}$$

where k_3 is a positive design parameter. Let $e_q = q - q_d$, $\varepsilon_q = q_d - q_d^c$, and substitute (24) into (23), we obtain

$$\begin{aligned} \dot{V}_2 &= e_\theta \left(\lambda_\theta (e_q + \varepsilon_q + q_d^c) + \kappa_\theta \dot{\theta}_d\right) \\ &= -k_3 \lambda_\theta e_\theta^2 + \lambda_\theta e_\theta (e_q + \varepsilon_q) - z_e e_\theta U \varphi\left(\tilde{\theta}, \chi\right). \end{aligned} \tag{25}$$

In the subsequent step, we need to design a virtual control law for x_c. However, the functions f_c and g_c are supposed to be unknown, which leads to the model-based approaches in [18] being unavailable in this case. To address this problem, we denote $\beta = \bar{g}_c/g_c$ and

define the Lyapunov function as $V_3 = V_2 + \int_0^{e_q} \frac{\beta\sigma\left(k_{lq}+k_{uq}\right)^2}{4\left(k_{lq}+\sigma+q_d\right)\left(k_{uq}-\sigma-q_d\right)} d\sigma$. Recalling Lemma 1 and Assumption 3, we have

$$\begin{aligned}\dot{V}_3 &= \dot{V}_2 + e_q\left(\beta\lambda_q\dot{q} - \rho\left(e_q, q_d\right)\dot{q}_d\right) \\ &= -k_3\lambda_\theta e_\theta^2 + \lambda_\theta e_\theta\varepsilon_q - z_e e_\theta U\varphi\left(\tilde{\theta}, \chi\right) \\ &\qquad + e_q\left(\lambda_\theta e_\theta + \lambda_q\left(\beta f_c + \bar{g}_c x_c + \beta d_q - \lambda_q^{-1}\rho\left(e_q, q_d\right)\dot{q}_d\right)\right).\end{aligned} \tag{26}$$

Let $h\left(\zeta\right) = \beta f_c - \lambda_q^{-1}\rho\left(e_q, q_d\right)\dot{q}_d$ and applying Lemma 2, we can approximate this function by $h\left(\zeta\right) = W^T S\left(\zeta\right) + \varepsilon_{NN}$. Inspired by [32], the following update law is constructed to estimate the ideal weight vector

$$\dot{\hat{W}} = \Gamma\left(e_q S\left(\zeta\right) - \mu_W\left|e_q\right|\hat{W}\right), \tag{27}$$

where $\hat{W}$ is the estimated value of W and $\Gamma > 0$, $\mu_W > 0$. If we choose the activation function as the Gaussian function, then there exists a positive constant b_S independent of the number of nodes and the inputs such that $\left\|S\left(\zeta\right)\right\| \leqslant b_S$ [33]. Moreover, according to [32], $\hat{W}$ is guaranteed to be bounded when $\left\|S\left(\zeta\right)\right\|$ is bounded. Thus, there exist a positive constant b_W such that $\left\|\tilde{W}\right\| = \left\|W - \hat{W}\right\| \leqslant b_W$. Denote $\delta = b_W b_S + \bar{\varepsilon}_{NN} + \bar{\beta}\bar{d}_q$, we can rewrite the equation (26) as

$$\begin{aligned}\dot{V}_3 &= -k_3\lambda_\theta e_\theta^2 + \lambda_\theta e_\theta\varepsilon_q - z_e e_\theta U\varphi\left(\tilde{\theta}, \chi\right) \\ &\qquad + e_q\left(\lambda_\theta e_\theta + \lambda_q\left(\hat{W}^T S\left(\zeta\right) + \bar{g}_c x_c + \tilde{W}^T S\left(\zeta\right) + \varepsilon_{NN} + \beta d_q\right)\right) \\ &\leqslant -k_3\lambda_\theta e_\theta^2 + \lambda_\theta e_\theta\varepsilon_q - z_e e_\theta U\varphi\left(\tilde{\theta}, \chi\right) \\ &\qquad + e_q\left(\lambda_\theta e_\theta + \lambda_q\left(\hat{W}^T S\left(\zeta\right) + \bar{g}_c x_c\right)\right) + \lambda_q\left|e_q\right|\delta.\end{aligned} \tag{28}$$

Besides, using Lemma 3, we have

$$-\lambda_q e_q\hat{\delta}\tanh\left(\frac{\lambda_q e_q\hat{\delta}}{\varsigma}\right) \leqslant -\left|\lambda_q e_q\hat{\delta}\right| + \eta\varsigma \leqslant -\lambda_q\left|e_q\right|\hat{\delta} + \eta\varsigma, \tag{29}$$

where $\hat{\delta}$ is the estimated value of δ. Select the virtual control law as

$$x_{cd}^c = \frac{-k_4 e_q - \hat{W}^T S\left(\zeta\right) - \lambda_q^{-1}\lambda_\theta e_\theta - \hat{\delta}\tanh\left(\frac{\lambda_q e_q\hat{\delta}}{\varsigma}\right)}{\bar{g}_c}, \tag{30}$$

where $k_4 > 0$. Let $e_{xc} = x_c - x_{cd}$, $\varepsilon_{xc} = x_{cd} - x_{cd}^c$, $\tilde{\delta} = \delta - \hat{\delta}$, and substitute (29) - (30) into

(28), we obtain

$$\begin{aligned}\dot{V}_3 \leqslant & -k_3\lambda_\theta e_\theta^2 + \lambda_\theta e_\theta \varepsilon_q - z_e e_\theta U\varphi\left(\tilde{\theta},\chi\right) \\ & + e_q\left(\lambda_\theta e_\theta + \lambda_q\left(\hat{W}^T S\left(\zeta\right) + \bar{g}_c\left(e_{xc} + \varepsilon_{xc} + x_{cd}^c\right)\right)\right) + \lambda_q\left|e_q\right|\delta \\ \leqslant & -k_3\lambda_\theta e_\theta^2 + \lambda_\theta e_\theta \varepsilon_q - z_e e_\theta U\varphi\left(\tilde{\theta},\chi\right) \\ & - k_4\lambda_q e_q^2 - \lambda_q e_q\hat{\delta}\tanh\left(\frac{\lambda_q e_q\hat{\delta}}{\varsigma}\right) + \lambda_q\bar{g}_c e_q\left(e_{xc}+\varepsilon_{xc}\right) + \lambda_q\left|e_q\right|\delta \\ \leqslant & -k_3\lambda_\theta e_\theta^2 - k_4\lambda_q e_q^2 + \lambda_\theta e_\theta\varepsilon_q - z_e e_\theta U\varphi\left(\tilde{\theta},\chi\right) \\ & + \lambda_q\left|e_q\right|\tilde{\delta} + \lambda_q\bar{g}_c e_q\left(e_{xc}+\varepsilon_{xc}\right) + \eta\varsigma.\end{aligned} \tag{31}$$

Consider the Lyapunov function candidate $V_4 = V_3 + \frac{1}{2\gamma}\tilde{\delta} + \int_0^{e_{xc}} \frac{\sigma(k_{lM}+k_{uM})^2}{4(k_{lM}+\sigma+x_{cd})(k_{uM}-\sigma-x_{cd})}d\sigma$ where γ is a positive design parameter. Differentiating V_4 with respect to time, we obtain

$$\begin{aligned}\dot{V}_4 &= \dot{V}_3 - \gamma^{-1}\tilde{\delta}\dot{\hat{\delta}} + e_{xc}\left(\lambda_{xc}\vartheta + \kappa_{xc}\dot{x}_{cd}\right) \\ &\leqslant -k_3\lambda_\theta e_\theta^2 - k_4\lambda_q e_q^2 + \lambda_\theta e_\theta\varepsilon_q + \lambda_q\bar{g}_c e_q\varepsilon_{xc} - z_e e_\theta U\varphi\left(\tilde{\theta},\chi\right) \\ &\quad + \tilde{\delta}\left(\lambda_q\left|e_q\right| - \gamma^{-1}\dot{\hat{\delta}}\right) + e_{xc}\left(\lambda_q\bar{g}_c e_q + \lambda_{xc}\vartheta + \kappa_{xc}\dot{x}_{cd}\right) + \eta\varsigma.\end{aligned} \tag{32}$$

Select the virtual control law and adaptive law as

$$\vartheta_d^c = -k_5 e_{xc} - \lambda_{xc}^{-1}\lambda_q\bar{g}_c e_q - \lambda_{xc}^{-1}\kappa_{xc}\dot{x}_{cd}, \tag{33a}$$

$$\dot{\hat{\delta}} = \gamma\left(\lambda_q\left|e_q\right| - \mu_\delta\hat{\delta}\right), \tag{33b}$$

where k_5, $\mu_\delta > 0$. Let $e_\vartheta = \vartheta - \vartheta_d$, $\varepsilon_\vartheta = \vartheta_d - \vartheta_d^c$, and substitute (33a) and (33b) into (32), we obtain

$$\begin{aligned}\dot{V}_4 \leqslant & -k_3\lambda_\theta e_\theta^2 - k_4\lambda_q e_q^2 - k_5\lambda_{xc}e_{xc}^2 + \lambda_\theta e_\theta\varepsilon_q + \lambda_q\bar{g}_c e_q\varepsilon_{xc} \\ & - z_e e_\theta U\varphi\left(\tilde{\theta},\chi\right) + \mu_\delta\tilde{\delta}\hat{\delta} + \lambda_{xc}e_{xc}\left(e_\vartheta + \varepsilon_\vartheta\right) + \eta\varsigma.\end{aligned} \tag{34}$$

Define the Lyapunov function as $V_5 = V_4 + \int_0^{e_\vartheta} \frac{\sigma(k_{lR}+k_{uR})^2}{4(k_{lR}+\sigma+\vartheta_d)(k_{uR}-\sigma-\vartheta_d)}d\sigma$, whose time derivative is

$$\begin{aligned}\dot{V}_5 &= \dot{V}_4 + e_\vartheta\left(\lambda_\vartheta\tau + \kappa_\vartheta\dot{\vartheta}_d\right) \\ &\leqslant -k_3\lambda_\theta e_\theta^2 - k_4\lambda_q e_q^2 - k_5\lambda_{xc}e_{xc}^2 + \lambda_\theta e_\theta\varepsilon_q + \lambda_q\bar{g}_c e_q\varepsilon_{xc} + \lambda_{xc}e_{xc}\varepsilon_\vartheta \\ &\quad - z_e e_\theta U\varphi\left(\tilde{\theta},\chi\right) + \mu_\delta\tilde{\delta}\hat{\delta} + e_\vartheta\left(\lambda_{xc}e_{xc} + \lambda_\vartheta\tau + \kappa_\vartheta\dot{\vartheta}_d\right) + \eta\varsigma.\end{aligned} \tag{35}$$

Select the control law as

$$\tau = -k_6 e_\vartheta - \lambda_\vartheta^{-1}\lambda_{xc}e_{xc} - \lambda_\vartheta^{-1}\kappa_\vartheta\dot{\vartheta}_d, \tag{36}$$

where $k_6 > 0$. Then

$$\begin{aligned}\dot{V}_5 \leqslant & -k_3\lambda_\theta e_\theta^2 - k_4\lambda_q e_q^2 - k_5\lambda_{xc}e_{xc}^2 - k_6\lambda_\vartheta e_\vartheta^2 \\ & + \lambda_\theta e_\theta\varepsilon_q + \lambda_q\bar{g}_c e_q\varepsilon_{xc} + \lambda_{xc}e_{xc}\varepsilon_\vartheta - z_e e_\theta U\varphi\left(\tilde{\theta},\chi\right) + \mu_\delta\tilde{\delta}\hat{\delta} + \eta\varsigma.\end{aligned} \tag{37}$$

3.3. Controller stability analysis

The stability of the closed-loop system is the focus of this section, and the following theorem provides a succinct summary of the results.

Theorem 1. *Consider a desired path* $p_d(\varpi) = [x_d(\varpi), z_d(\varpi)]^T$ *with the path variable* ϖ *being updated by (18a). Then under Assumptions 1 - 4 and any bounded initial conditions satisfying (6), the guidance law (18b), the control laws (24), (30), (33a), (36), and the adaptive laws (27), (33b) guarantee that*

(i) The path-following errors are ultimately uniformly bounded (UUB).

(ii) The constraints (6) are never violated.

Proof.

(i) Let a Lyapunov function candidate for the closed-loop system be $V = V_1 + V_5 + \frac{1}{2}\sum_{i=\theta,q,xc,\vartheta}\varepsilon_i^2$ where $\varepsilon_\theta = \theta_d - \theta_d^c$. Differentiating V along (19), (21), (37) and note that $\tilde{\theta} = e_\theta + \varepsilon_\theta$, $\tilde{\delta}\hat{\delta} = \tilde{\delta}\left(\delta - \tilde{\delta}\right) \leqslant \left(\delta^2 - \tilde{\delta}^2\right)\big/2$, we have

$$\begin{aligned}\dot{V} \leqslant & -k_1 x_e^2 - k_2 z_e^2 - k_3\lambda_\theta e_\theta^2 - k_4\lambda_q e_q^2 - k_5\lambda_{xc} e_{xc}^2 - k_6\lambda_\vartheta e_\vartheta^2 - \frac{\mu_\delta}{2}\tilde{\delta}^2 + \frac{\mu_\delta}{2}\delta^2 + \eta\varsigma \\ & + \sum_{i=\theta,q,xc,\vartheta}\varepsilon_i\left(-\frac{1}{T_i}\varepsilon_i + \Delta H_i - \dot{i}_d^c\right) + \lambda_\theta e_\theta\varepsilon_q + \lambda_q\bar{g}_c e_q\varepsilon_{xc} + \lambda_{xc}e_{xc}\varepsilon_\vartheta + z_e\varepsilon_\theta U\varphi\left(\tilde{\theta},\chi\right),\end{aligned} \tag{38}$$

where $\Delta H_i = (H_i(i_d^c) - i_d^c)/T_i$. According to Young's inequality, the following inequalities holds

$$z_e\varepsilon_\theta U\varphi\left(\tilde{\theta},\chi\right) \leqslant \frac{\alpha_1}{4}z_e^2 + \frac{1}{\alpha_1}U^2\varepsilon_\theta^2, \tag{39a}$$

$$\lambda_\theta e_\theta\varepsilon_q \leqslant \lambda_\theta\left(\frac{\alpha_2}{4}e_\theta^2 + \frac{1}{\alpha_2}\varepsilon_q^2\right), \tag{39b}$$

$$\lambda_q\bar{g}_c e_q\varepsilon_{xc} \leqslant \lambda_q\left(\frac{\alpha_3}{4}e_q^2 + \frac{1}{\alpha_3}\bar{g}_c^2\varepsilon_{xc}^2\right), \tag{39c}$$

$$\lambda_{xc}e_{xc}\varepsilon_\vartheta \leqslant \lambda_{xc}\left(\frac{\alpha_4}{4}e_{xc}^2 + \frac{1}{\alpha_4}\varepsilon_\vartheta^2\right), \tag{39d}$$

$$\varepsilon_i\left(\Delta H_i - \dot{i}_d^c\right) \leqslant \frac{\alpha_5}{4}\varepsilon_i^2 + \frac{1}{\alpha_5}(\Delta H_i)^2 + \frac{\alpha_5}{4}\left(\varepsilon_i\dot{i}_d^c\right)^2 + \frac{1}{\alpha_5}. \tag{39e}$$

Define a compact set $\Xi = \left\{\left(x_e, z_e, e_\theta, e_q, e_{xc}, e_\vartheta, \tilde{\delta}, \varepsilon_\theta, \varepsilon_q, \varepsilon_{xc}, \varepsilon_\vartheta\right) : V \leqslant B_0\right\}$ with B_0 is a positive constant and $\Delta_V = \sum_{i=\theta,q,xc,\vartheta}\left((\Delta H_i)^2 + 1\right)\big/\alpha_5$. Employing the induction similar to [20, 34], we can infer that $\left|\dot{i}_d^c\right|$ $(i = \theta, q, x_c, \vartheta)$ has a maxima b_i on Ξ and there

exists b_Δ such that $b_\Delta \geqslant \Delta_V$. Select the time constants such that

$$\begin{cases} \dfrac{1}{T_\theta} & \geq \dfrac{U^2}{\alpha_1} + \dfrac{\alpha_5}{4} + \dfrac{\alpha_5}{4} b_\theta^2 + \eta_\theta \\ \dfrac{1}{T_q} & \geq \dfrac{\lambda_\theta}{\alpha_2} + \dfrac{\alpha_5}{4} + \dfrac{\alpha_5}{4} b_q^2 + \eta_q \\ \dfrac{1}{T_{xc}} & \geq \dfrac{\lambda_q \bar{g}_c^2}{\alpha_3} + \dfrac{\alpha_5}{4} + \dfrac{\alpha_5}{4} b_{xc}^2 + \eta_{xc} \\ \dfrac{1}{T_\vartheta} & \geq \dfrac{\lambda_{xc}}{\alpha_4} + \dfrac{\alpha_5}{4} + \dfrac{\alpha_5}{4} b_\vartheta^2 + \eta_\vartheta, \end{cases} \tag{40}$$

where $\eta_i \, (i = \theta, q, x_c, \vartheta)$ are positive constants. Then, (38) can be further expressed as

$$\begin{aligned} \dot{V} \leqslant & -k_1 x_e^2 - \left(k_2 - \frac{\alpha_1}{4}\right) z_e^2 - \lambda_\theta \left(k_3 - \frac{\alpha_2}{4}\right) e_\theta^2 - \lambda_q \left(k_4 - \frac{\alpha_3}{4}\right) e_q^2 \\ & - \lambda_{xc} \left(k_5 - \frac{\alpha_4}{4}\right) e_{xc}^2 - k_6 \lambda_\vartheta e_\vartheta^2 - \sum_{i=\theta,q,xc,\vartheta} \eta_i \varepsilon_i^2 \\ & - \frac{\mu_\delta}{2} \tilde{\delta}^2 + \frac{\mu_\delta}{2} \delta^2 + \eta\varsigma + b_\Delta \\ \leqslant & -k_V V + C_V, \end{aligned} \tag{41}$$

where $k_V = \min\left\{2k_1, 2\left(k_2 - \alpha_1/4\right), \left(k_3 - \alpha_2/4\right), \bar{\beta}^{-1}\left(k_4 - \alpha_3/4\right), \mu_\delta\gamma, \left(k_5 - \alpha_4/4\right), k_6, 2\eta_\theta, 2\eta_q, 2\eta_{xc}, 2\eta_\vartheta\right\}$, $C_V = \mu_\delta \delta^2/2 + \eta\varsigma + b_\Delta$. Besides, using Lemma 1, it can be inferred that

$$V \geqslant \frac{1}{2}\left(x_e^2 + z_e^2 + e_\theta^2 + e_q^2 + e_{xc}^2 + \gamma^{-1}\tilde{\delta}^2 + e_\vartheta^2 + \sum_{i=\theta,q,xc,\vartheta} \varepsilon_i^2\right). \tag{42}$$

By solving (41), we get

$$V(t) \leqslant \left(V(0) - \frac{C_V}{k_V}\right) e^{-k_V t} + \frac{C_V}{k_V}, \tag{43}$$

which implies that $V(t)$ is bounded and eventually resides inside a compact set $\Omega := \{V : V \leqslant C_V/k_V\}$. Combining this result with (42), we can conclude that the path-following errors are UUB.

(ii) We will prove this property by contradiction. Suppose that there exists a moment when the constraint state exceeds the boundary. Then, the corresponding IBLF will be infinite. This is in contrast to the above property that V is bounded. Consequently, it can be concluded that the constraints (6) are guaranteed. ∎

Remark 4. *From (43), we know that the larger k_V is, the faster the convergence can be achieved. However, simply trying to increase the control parameters will result in unexpected large control signals, which may cause system instability. Based on our experience developing control laws and personal experience, we propose the following guidelines for users during the parameter tuning process. From Figure 2, (18a) and (18b), it is intuitive to set a large k_1 to make x_e fast converge to 0, while Δ could be chosen based on the speed of the vehicle to avoid oscillation of the desired pitch angle. The control gains $k_i \, (i = 3, 4, 5, 6)$ should not be*

too large and have increasing value with each step. This will help ensure that the subsequent state can adhere to the virtual control variable calculated in the previous step. Regarding the adaptive parameters, users should adjust the magnitude of these parameters based on the trade-off between convergence rate and stability during the transition period.

4. SIMULATION RESULTS AND DISCUSSIONS

To verify the efficacy and feasibility of the designed controller, numerical simulation results via Matlab/Simulink and related discussion are carried out in this section. The model parameters are taken from [14]. In the simulation scenario, the vehicle is required to follow a desired parameterized path $p_d(\varpi) = [1.5\varpi, 20 + 1.5\sin(0.1\varpi)]^\top$ with $\varpi(0) = 0$ under the external disturbances $d_u = 0.01\sin(\pi t/20)$, $d_w = 0.01\sin(\pi t/20)$, $d_q = 0.03 + 0.01\sin(\pi t/20)$. The initial conditions are assigned as $[x(0), z(0), \theta(0)]^\top = [u(0), w(0), q(0)]^\top = [0,0,0]^\top$, $x_G(0) = \dot{x}_G(0) = 0$. The physical constraints are set to $k_{lM} = 0$, $k_{uM} = 20$, $k_{lR} = k_{uR} = 10$, $k_{l\theta} = 15\pi/36$, $k_{u\theta} = 4\pi/9$, $k_{lq} = k_{uq} = \pi/12$. The control gains are selected as $k_1 = 20$, $\Delta = 3$, $k_3 = 0.3$, $k_4 = 0.8$, $k_5 = 1$, $k_6 = 5$. To overcome the complex uncertainties, including unknown dynamic parameters and disturbances, we use the RBF NN with eight nodes, centers evenly spaced in $[-5, 5]$, and widths of 1. The adaptive parameters are selected as $\hat{W}(0) = 0$, $\Gamma = 10$, $\mu_W = 0.1$, $\hat{\delta}(0) = 0$, $\gamma = 1$, $\mu_\delta = 0.01$.

To highlight the benefits of the suggested method, we make a comparison with the backstepping controller suggested in [18]. In particular, the control and adaptive laws are modified as follows

$$q_d = -k_3 e_\theta + \dot{\theta}_d - z_e U \varphi(e_\theta, \chi), \tag{44a}$$

$$x_{cd} = \frac{-k_4 e_q - \hat{W}^T S(\zeta) - e_\theta - \hat{\delta}\tanh\left(\frac{e_q\hat{\delta}}{\varsigma}\right)}{\bar{g}_c}, \tag{44b}$$

$$\dot{\hat{\delta}} = \gamma\left(|e_q| - \mu_\delta\hat{\delta}\right). \tag{44c}$$

The simulation results are depicted in Figures 3 to 6. Figure 3a shows the path-following results of the proposed controller and the backstepping controller. Therein, the constrained backstepping (CBC) and unconstrained backstepping (UBC) stand for the performance of the backstepping controller with and without the input constraints, respectively. It can be observed that the backstepping controller can work consistently without the input constraints; otherwise, the response fluctuates, causing a significant reduction in performance. The path-following errors are presented in Figure 3b, demonstrating that the proposed controller can force the errors to converge to a small neighborhood of zero with a smooth transient performance regardless of unknown model information and external disturbances. Moreover, to make the insight comparisons, Table 1 presents the integrated absolute error (IAE), the integrated time absolute error (ITAE), and the integral of square error (ISA), which relate the transient performance, the steady-state performance, and the control energy, respectively. As can be seen in Table 1, CBC has the worst performance in all criteria because its response fluctuates, and UBC has an IAE slightly smaller than the proposed controller since it has no constraint on control input. Otherwise, the proposed method has the smallest ITAE and ISA, which means it has the best steady-state performance and lowest control energy consumption. Figures 4 and 5 point out that except for pitch angle, all other constraints are

violated by the UBC, while the proposed method guarantees that all constrained states remain within the given boundary. This property enables the designed controller to efficiently comply with the physical characteristics of the actual model, thus increasing practical application. Figure 6 depicts the evolution of RBF NN weights, showing that NN weights converge after about 50s, which is close to the time when the error z_e converges to 0. It is noticed that guaranteeing the constraints on system states can solve safety-related problems in many applications [35]. Therefore, extending the proposed algorithm into a general one is interesting.

Table 1: Performance comparisons among three controllers

Controller	IAE $\int_0^t \lvert z_e \rvert \, d\tau$	ITAE $\int_0^t \tau \lvert z_e \rvert \, d\tau$	ISA $\int_0^t x_c^2 d\tau \times 10^4$
UBC	241.7	2589	3.623
CBC	293.1	5312	3.726
Proposed	256.9	2477	2.742

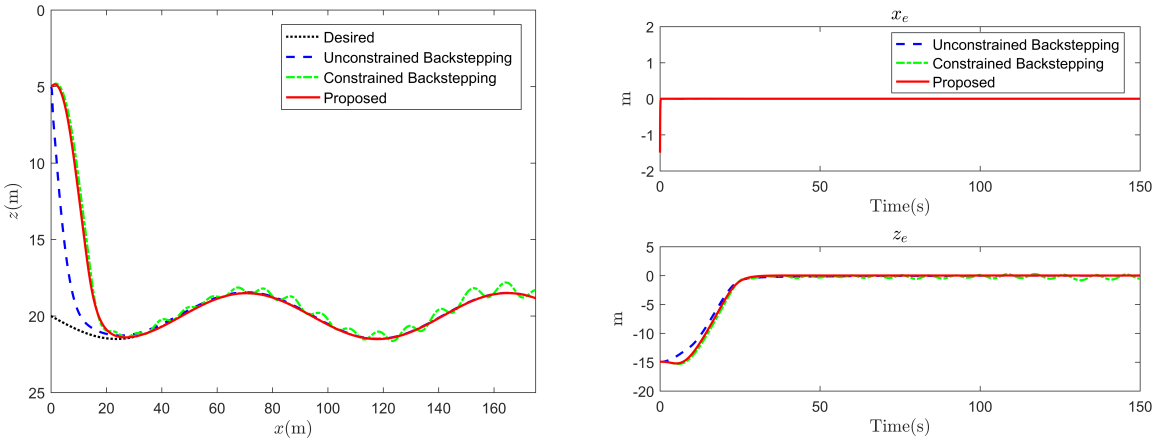

(a) (b)

Figure 3: Comparison of path-following performance of different controllers

5. CONCLUSION

This study addresses the path-following control for under-actuated AUVs subject to system uncertainties, external disturbances, and physical constraints. By developing a novel IBLF and using a dexterous transformation, the proposed method could augment with RBF NN to simultaneously solve state constraint problems, input saturations, and unknown model coefficients. The adaptive technique is also incorporated into the design procedure to handle disturbances and enhance the controller's robustness. Theoretical proof and simulation results are strong evidence that verifies the superiority of the suggested approach compared to the previous ones.

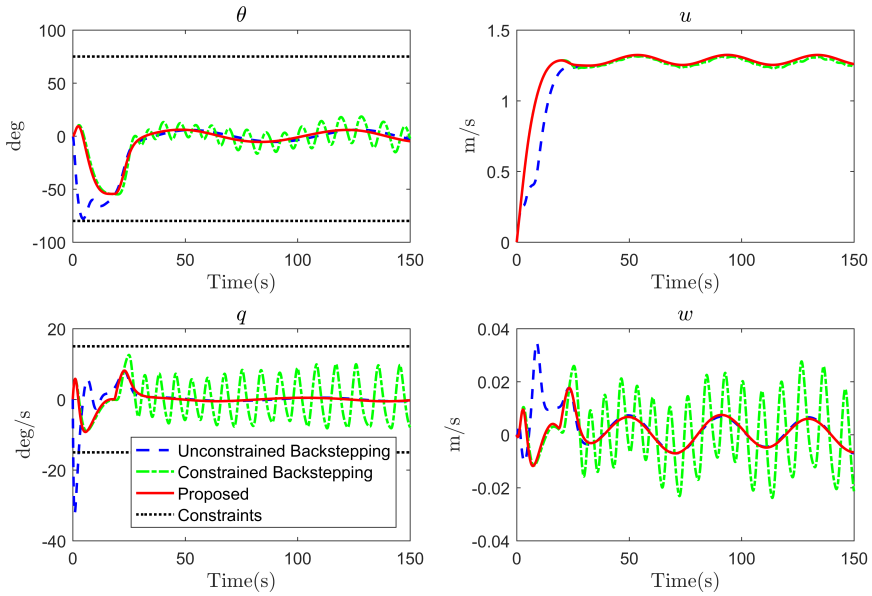

Figure 4: State response of different controllers

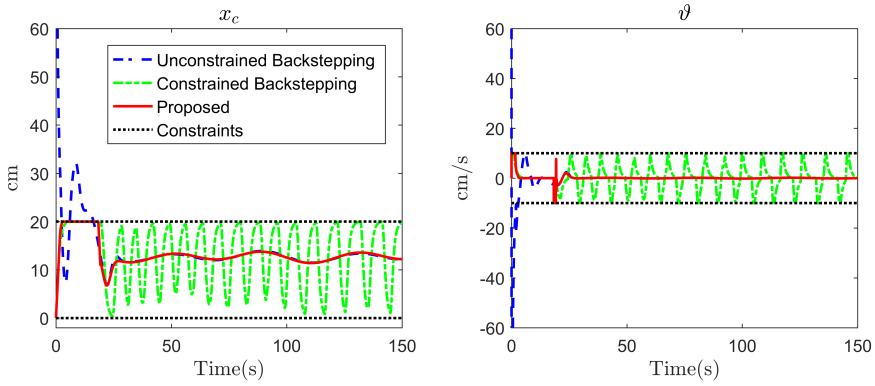

Figure 5: Control inputs of different controllers

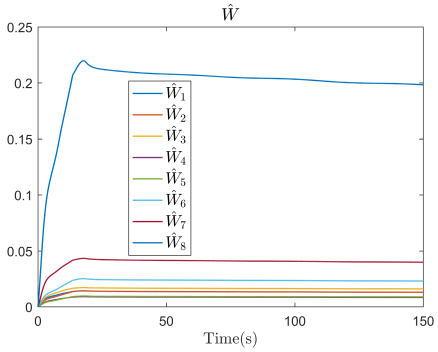

Figure 6: The evolution of RBF NN weights

ACKNOWLEDGMENT

This research is funded by Vietnam National Foundation for Science and Technology Development (NAFOSTED), Vietnam, under grant number MDT 107.01-2021.22.

Pham Nguyen Nhut Thanh was funded by the Master, PhD Scholarship Programme of Vingroup Innovation Foundation (VINIF), code VINIF.2023.TS.110.

We acknowledge Ho Chi Minh City University of Technology (HCMUT), VNU-HCM for supporting this study.

REFERENCES

[1] Y. Shi, C. Shen, H. Fang, and H. Li, "Advanced control in marine mechatronic systems: A survey," *IEEE/ASME Transactions on Mechatronics*, vol. 22, no. 3, pp. 1121–1131, Jun. 2017. [Online]. Available: http://dx.doi.org/10.1109/TMECH.2017.2660528

[2] E. Zereik, M. Bibuli, N. Mišković, P. Ridao, and A. Pascoal, "Challenges and future trends in marine robotics," *Annual Reviews in Control*, vol. 46, pp. 350–368, 2018. [Online]. Available: http://dx.doi.org/10.1016/j.arcontrol.2018.10.002

[3] Y. Yang, Y. Xiao, and T. Li, "A survey of autonomous underwater vehicle formation: Performance, formation control, and communication capability," *IEEE Communications Surveys & Tutorials*, vol. 23, no. 2, pp. 815–841, 2021. [Online]. Available: http://dx.doi.org/10.1109/COMST.2021.3059998

[4] Z. Peng and J. Wang, "Output-feedback path-following control of autonomous underwater vehicles based on an extended state observer and projection neural networks," *IEEE Transactions on Systems, Man, and Cybernetics: Systems*, vol. 48, no. 4, pp. 535–544, Apr. 2018. [Online]. Available: http://dx.doi.org/10.1109/TSMC.2017.2697447

[5] P. N. Nhut Thanh, P. M. Tam, and H. P. Huy Anh, "A new approach for three-dimensional trajectory tracking control of under-actuated auvs with model uncertainties," *Ocean Engineering*, vol. 228, p. 108951, May 2021. [Online]. Available: http://dx.doi.org/10.1016/j.oceaneng.2021.108951

[6] L. Lapierre and B. Jouvencel, "Robust nonlinear path-following control of an auv," *IEEE Journal of Oceanic Engineering*, vol. 33, no. 2, pp. 89–102, Apr. 2008. [Online]. Available: http://dx.doi.org/10.1109/JOE.2008.923554

[7] E. Peymani and T. I. Fossen, "Path following of underwater robots using lagrange multipliers," *Robotics and Autonomous Systems*, vol. 67, pp. 44–52, May 2015. [Online]. Available: http://dx.doi.org/10.1016/j.robot.2014.10.011

[8] J. Yu, J. Liu, Z. Wu, and H. Fang, "Depth control of a bioinspired robotic dolphin based on sliding-mode fuzzy control method," *IEEE Transactions on Industrial Electronics*, vol. 65, no. 3, pp. 2429–2438, Mar. 2018. [Online]. Available: http://dx.doi.org/10.1109/TIE.2017.2745451

[9] M. Lei, "Nonlinear diving stability and control for an auv via singular perturbation," *Ocean Engineering*, vol. 197, p. 106824, Feb. 2020. [Online]. Available: http://dx.doi.org/10.1016/j.oceaneng.2019.106824

[10] D. Belleter, M. A. Maghenem, C. Paliotta, and K. Y. Pettersen, "Observer based path following for underactuated marine vessels in the presence of ocean currents: A global approach," *Automatica*, vol. 100, pp. 123–134, Feb. 2019. [Online]. Available: http://dx.doi.org/10.1016/j.automatica.2018.11.008

[11] P. N. N. Thanh and H. P. H. Anh, "Neural network-based depth and horizontal control for autonomous underwater vehicles with prescribed performance," *Ocean Engineering*, vol. 281, p. 114647, Aug. 2023. [Online]. Available: http://dx.doi.org/10.1016/j.oceaneng.2023.114647

[12] Z. Zheng and L. Sun, "Path following control for marine surface vessel with uncertainties and input saturation," *Neurocomputing*, vol. 177, pp. 158–167, Feb. 2016. [Online]. Available: http://dx.doi.org/10.1016/j.neucom.2015.11.017

[13] T. I. Fossen and A. M. Lekkas, "Direct and indirect adaptive integral line-of-sight path-following controllers for marine craft exposed to ocean currents," *International Journal of Adaptive Control and Signal Processing*, vol. 31, no. 4, pp. 445–463, Mar. 2015. [Online]. Available: http://dx.doi.org/10.1002/acs.2550

[14] P. N. N. Thanh, N. A. Thuyen, and H. P. H. Anh, "Adaptive fuzzy 3-d trajectory tracking control for autonomous underwater vehicle (auv) using modified integral barrier lyapunov function," *Ocean Engineering*, vol. 283, p. 115027, Sep. 2023. [Online]. Available: http://dx.doi.org/10.1016/j.oceaneng.2023.115027

[15] J. Miao, S. Wang, M. M. Tomovic, and Z. Zhao, "Compound line-of-sight nonlinear path following control of underactuated marine vehicles exposed to wind, waves, and ocean currents," *Nonlinear Dynamics*, vol. 89, no. 4, pp. 2441–2459, Jun. 2017. [Online]. Available: http://dx.doi.org/10.1007/s11071-017-3596-9

[16] Y. Su, L. Wan, D. Zhang, and F. Huang, "An improved adaptive integral line-of-sight guidance law for unmanned surface vehicles with uncertainties," *Applied Ocean Research*, vol. 108, p. 102488, Mar. 2021. [Online]. Available: http://dx.doi.org/10.1016/j.apor.2020.102488

[17] K. Do, "Global robust adaptive path-tracking control of underactuated ships under stochastic disturbances," *Ocean Engineering*, vol. 111, pp. 267–278, Jan. 2016. [Online]. Available: http://dx.doi.org/10.1016/j.oceaneng.2015.10.038

[18] H. N. Tran, T. N. Nhut Pham, and S. H. Choi, "Robust depth control of a hybrid autonomous underwater vehicle with propeller torque's effect and model uncertainty," *Ocean Engineering*, vol. 220, p. 108257, Jan. 2021. [Online]. Available: http://dx.doi.org/10.1016/j.oceaneng.2020.108257

[19] Z. Zheng and M. Feroskhan, "Path following of a surface vessel with prescribed performance in the presence of input saturation and external disturbances,"

IEEE/ASME Transactions on Mechatronics, vol. 22, no. 6, pp. 2564–2575, Dec. 2017. [Online]. Available: http://dx.doi.org/10.1109/TMECH.2017.2756110

[20] K. D. von Ellenrieder, "Dynamic surface control of trajectory tracking marine vehicles with actuator magnitude and rate limits," *Automatica*, vol. 105, pp. 433–442, Jul. 2019. [Online]. Available: http://dx.doi.org/10.1016/j.automatica.2019.04.018

[21] J. Zhang, X. Xiang, Q. Zhang, and W. Li, "Neural network-based adaptive trajectory tracking control of underactuated auvs with unknown asymmetrical actuator saturation and unknown dynamics," *Ocean Engineering*, vol. 218, p. 108193, Dec. 2020. [Online]. Available: http://dx.doi.org/10.1016/j.oceaneng.2020.108193

[22] C. Yu, X. Xiang, P. A. Wilson, and Q. Zhang, "Guidance-error-based robust fuzzy adaptive control for bottom following of a flight-style auv with saturated actuator dynamics," *IEEE Transactions on Cybernetics*, vol. 50, no. 5, pp. 1887–1899, May 2020. [Online]. Available: http://dx.doi.org/10.1109/TCYB.2018.2890582

[23] T. I. Fossen, *Handbook of Marine Craft Hydrodynamics and Motion Control*. Wiley, Apr. 2011. [Online]. Available: http://dx.doi.org/10.1002/9781119994138

[24] M. Chen, S. S. Ge, and B. Ren, "Adaptive tracking control of uncertain mimo nonlinear systems with input constraints," *Automatica*, vol. 47, no. 3, pp. 452–465, Mar. 2011. [Online]. Available: http://dx.doi.org/10.1016/j.automatica.2011.01.025

[25] A. Zou, K. D. Kumar, and A. H. J. de Ruiter, "Robust attitude tracking control of spacecraft under control input magnitude and rate saturations," *International Journal of Robust and Nonlinear Control*, vol. 26, no. 4, pp. 799–815, Mar. 2015. [Online]. Available: http://dx.doi.org/10.1002/rnc.3338

[26] Z.-L. Tang, S. S. Ge, K. P. Tee, and W. He, "Robust adaptive neural tracking control for a class of perturbed uncertain nonlinear systems with state constraints," *IEEE Transactions on Systems, Man, and Cybernetics: Systems*, vol. 46, no. 12, pp. 1618–1629, Dec. 2016. [Online]. Available: http://dx.doi.org/10.1109/TSMC.2015.2508962

[27] T. Prestero, *Verification of a six-degree of freedom simulation model for the REMUS autonomous underwater vehicle*. Massachusetts Institute of Technology and Woods Hole Oceanographic Institution, 2001. [Online]. Available: http://dx.doi.org/10.1575/1912/3040

[28] S. Ge, C. Hang, and T. Zhang, "Stable adaptive control for nonlinear multivariable systems with a triangular control structure," *IEEE Transactions on Automatic Control*, vol. 45, no. 6, pp. 1221–1225, Jun. 2000. [Online]. Available: http://dx.doi.org/10.1109/9.863612

[29] P. N. N. Thanh and H. P. H. Anh, "Advanced neural control technique for autonomous underwater vehicles using modified integral barrier lyapunov function," *Ocean Engineering*, vol. 266, p. 112842, Dec. 2022. [Online]. Available: http://dx.doi.org/10.1016/j.oceaneng.2022.112842

[30] J. Park and I. W. Sandberg, "Universal approximation using radial-basis-function networks," *Neural Computation*, vol. 3, no. 2, pp. 246–257, Jun. 1991. [Online]. Available: http://dx.doi.org/10.1162/neco.1991.3.2.246

[31] M. Polycarpou, "Stable adaptive neural control scheme for nonlinear systems," *IEEE Transactions on Automatic Control*, vol. 41, no. 3, pp. 447–451, Mar. 1996. [Online]. Available: http://dx.doi.org/10.1109/9.486648

[32] S. Huang, K. Tan, and T. Lee, "Further results on adaptive control for a class of nonlinear systems using neural networks," *IEEE Transactions on Neural Networks*, vol. 14, no. 3, pp. 719–722, May 2003. [Online]. Available: http://dx.doi.org/10.1109/TNN.2003.811712

[33] A. J. Kurdila, F. J. Narcowich, and J. D. Ward, "Persistency of excitation in identification using radial basis function approximants," *SIAM Journal on Control and Optimization*, vol. 33, no. 2, pp. 625–642, Mar. 1995. [Online]. Available: http://dx.doi.org/10.1137/S0363012992232555

[34] D. Swaroop, J. Hedrick, P. Yip, and J. Gerdes, "Dynamic surface control for a class of nonlinear systems," *IEEE Transactions on Automatic Control*, vol. 45, no. 10, pp. 1893–1899, Oct. 2000. [Online]. Available: http://dx.doi.org/10.1109/TAC.2000.880994

[35] Z. Peng, J. Li, B. Han, and N. Gu, "Safety-certificated line-of-sight guidance of unmanned surface vehicles for straight-line following in a constrained water region subject to ocean currents," *Journal of Marine Science and Application*, vol. 22, no. 3, pp. 602–613, Sep. 2023. [Online]. Available: http://dx.doi.org/10.1007/s11804-023-00351-9

Received on December 04, 2023
Accepted on June 03, 2024